SUPPLEMENTARY MATERIAL 2

In vitro Antibacterial Susceptibility of Different Pathogens to Thirty Nano-Polyoxometalates

Ștefana Bâlici[a], Dan Rusu[b], Emőke Páll[c], Miuța Filip[d], Flore Chirilă[e], Gheorghe Zsolt Nicula[a], Mihaela Laura Vică[a,*], Rodica Ungur[f], Horea-Vladi Matei[a], Nicodim Iosif Fiț[e]

[a] "Iuliu Haţieganu" University of Medicine and Pharmacy, Faculty of Medicine, Department of Cell and Molecular Biology, Cluj-Napoca, România
[b] "Iuliu Haţieganu" University of Medicine and Pharmacy, Faculty of Pharmacy, Department of Physical-Chemistry, Cluj-Napoca, România
[c] University of Agricultural Science and Veterinary Medicine, Faculty of Veterinary Medicine, Department of Reproduction, Obstetrics and Veterinary Gynecology, Cluj-Napoca, România
[d] "Babeș-Bolyai" University, "Raluca Ripan" Institute for Research in Chemistry, Analytical and Environmental Chemistry Laboratory, Cluj-Napoca, România
[e] University of Agricultural Science and Veterinary Medicine, Faculty of Veterinary Medicine, Department of Microbiology and Immunology, Cluj-Napoca, România
[f] "Iuliu Haţieganu" University of Medicine and Pharmacy, Faculty of Medicine, Department of Medical Rehabilitation, Cluj-Napoca, România
* Correspondence: mvica@umfcluj.ro

Supplemental Table of Contents

FTIR vibrational spectra of 27 nanoPOMs (Figures S6 – S32) 3
Figures S6 – S9. FTIR spectra of nanoPOMs with saturated Keggin structures 3
Figures S10 – S15. FTIR spectra of nanoPOMs with mono-lacunary Keggin structures 5
Figures S16 – S18. FTIR spectra of nanoPOMs with tri-lacunary Keggin structures 8
Figure S19. FTIR spectrum of nanoPOM with tri-lacunary *pseudo*-Keggin structures 9
Figures S20 –S23. FTIR spectra of nanoPOMs with tri-lacunary Keggin/sandwich type structures 10
Figures S24 – S26. FTIR spectra of nanoPOMs with tri-lacunary *pseudo*-Keggin/sandwich type structures 12
Figures S27 – S31. FTIR spectra of nanoPOMs with cluster structures 13
Figure S32. FTIR spectrum of nanoPOM, mono-lacunary Wells-Dawson with mixed addenda atoms 16

UV electronic spectra of 27 nanoPOMs (Figures S33 – S59) **17**
Figure S33 – S36. UV electronic spectra of nanoPOMs with saturated Keggin structures **17**
Figure S37 – S42. UV electronic spectra of nanoPOMs with mono-lacunary Keggin structures **18**
Figure S43 – S45. UV electronic spectra of nanoPOMs with tri-lacunary Keggin structures **19**
Figure S46. UV electronic spectrum of nanoPOM with tri-lacunary *pseudo*-Keggin structures **20**
Figure S47 – S50. UV electronic spectra of nanoPOMs with tri-lacunary Keggin/sandwich type structures **20**
Figure S51 – S53. UV electronic spectra of nanoPOMs with tri-lacunary *pseudo*-Keggin/sandwich type structures **22**
Figure S54 – S58. UV electronic spectra of nanoPOMs with cluster structures **23**
Figure S59. UV electronic spectrum of nanoPOM, mono-lacunary Wells-Dawson with mixed addenda atoms **24**

Bacterial inoculi microplates prepared from various reference strains inhibited by the 21 analyzed nanoPOMs (Figures S60 – S64) **25**
Figure S60. Inhibition aspects for the 21 nanoPOMs analyzed (in microplates of bacterial inoculum prepared from reference strain ATCC 6538P– *Staphylococcus aureus*): A-C. Active nanoPOMs, D. Control samples. **25**
Figure S61. Inhibition aspects for the 21 nanoPOMs analyzed (in microplates of bacterial inoculum prepared from reference strain ATCC 14579 – *Bacillus cereus*): A-C. Active nanoPOMs, D. Control samples. **25**
Figure S62. Inhibition aspects for the 21 nanoPOMs analyzed (in microplates of bacterial inoculum prepared from reference strain ATCC 13076 – *Salmonella enteritidis*): A-C. Active nanoPOMs, D. Control samples. **26**
Figure S63. Inhibition aspects for the 21 nanoPOMs analyzed (in microplates of bacterial inoculum prepared from reference strain ATCC 10536 – *Escherichia coli*): A-C. Active nanoPOMs, D. Control samples. **26**
Figure S64. Inhibition aspects for the 21 nanoPOMs analyzed (in microplates of bacterial inoculum prepared from reference strain ATCC 27853 – *Pseudomonas aeruginosa*): A-C. Active nanoPOMs, D. Control samples. **27**

FTIR vibrational spectra of 27 nanoPOMs

FTIR spectra of nanoPOMs with saturated Keggin structures

Figure S6. FTIR spectrum of POM 12, $H_4[SiW_{12}O_{40}]\cdot 14H_2O$

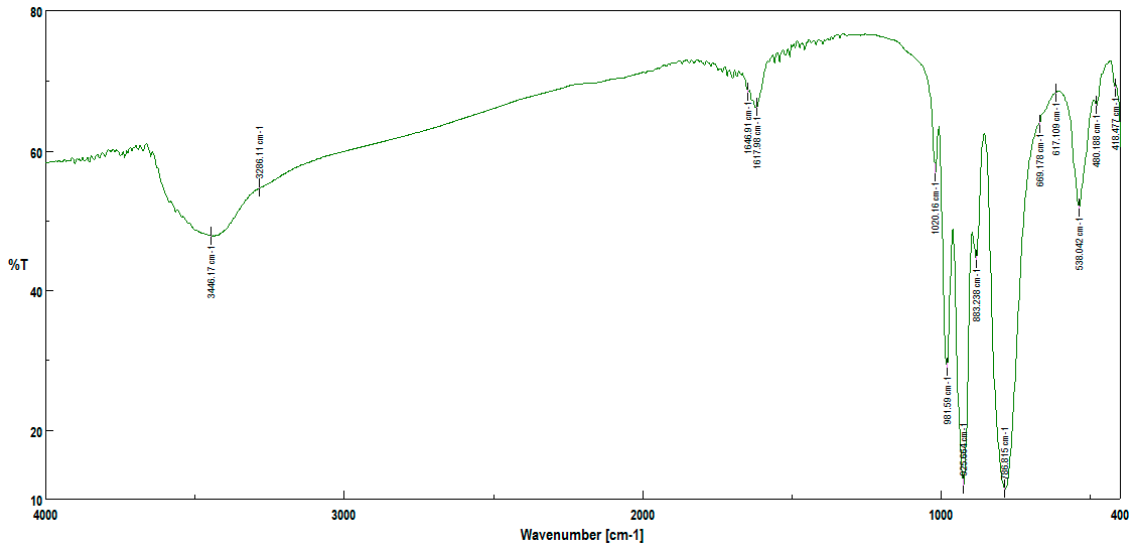

Figure S7. FTIR spectrum of POM 13, $H_3[PW_{12}O_{40}]\cdot 12H_2O$

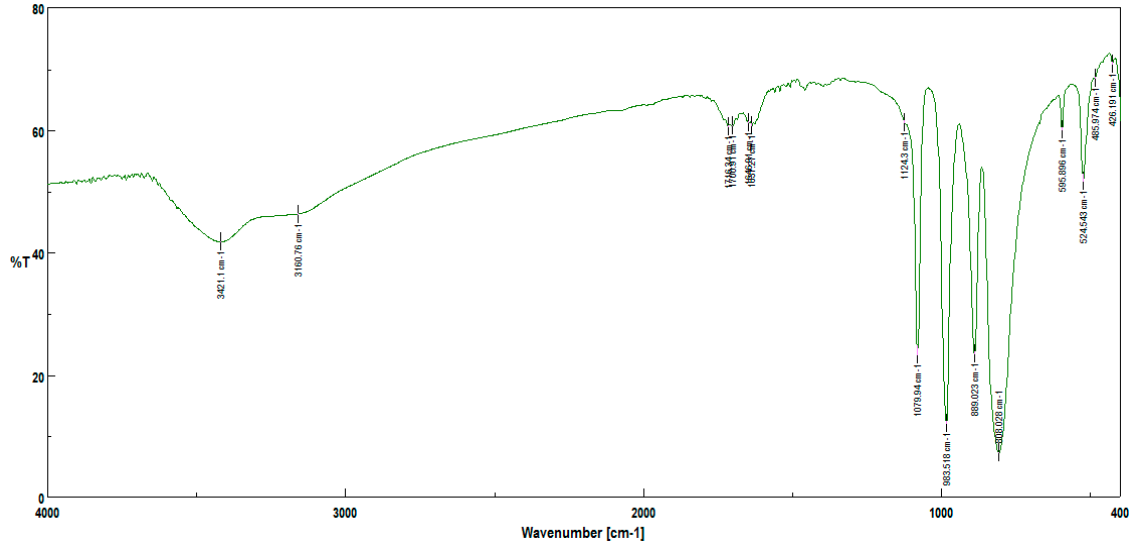

Figure S8. FTIR spectrum of POM 14, $H_3[PMo_{12}O_{40}]\cdot 13H_2O$

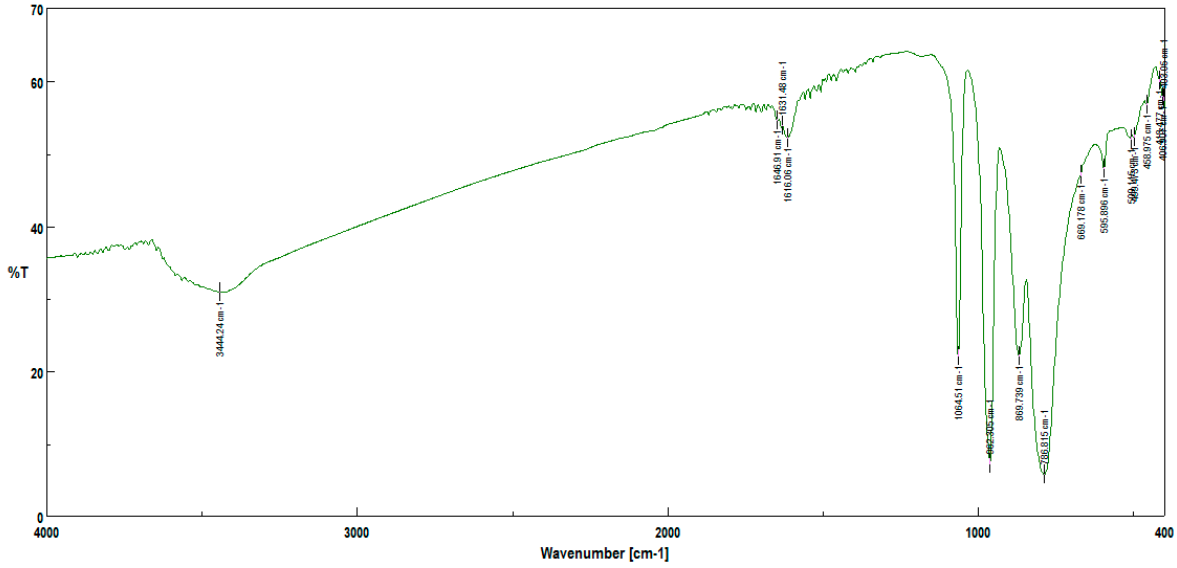

Figure S9. FTIR spectrum of POM 6, $Na_6[PMo_9^{VI}V_3^{V}O_{40}]\cdot 16H_2O$, Keggin with mixed addenda atoms

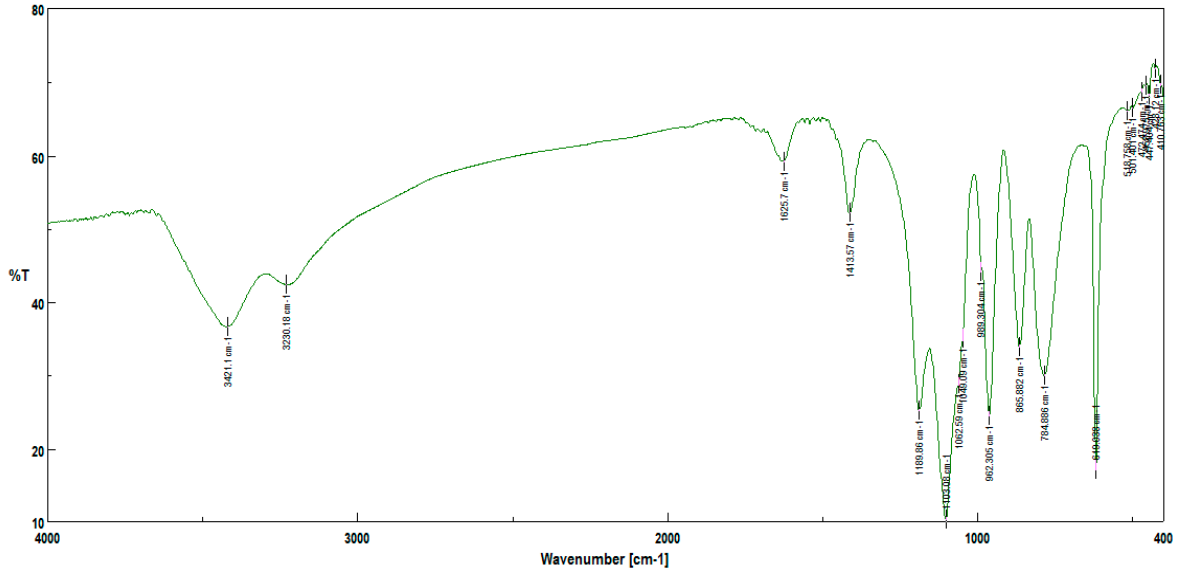

FTIR spectra of nanoPOMs with mono-lacunary Keggin structures

Figure S10. FTIR spectrum of POM 1, $Na_4[Fe^{III}(H_2O)PMo_{11}O_{39}]\cdot 18H_2O$

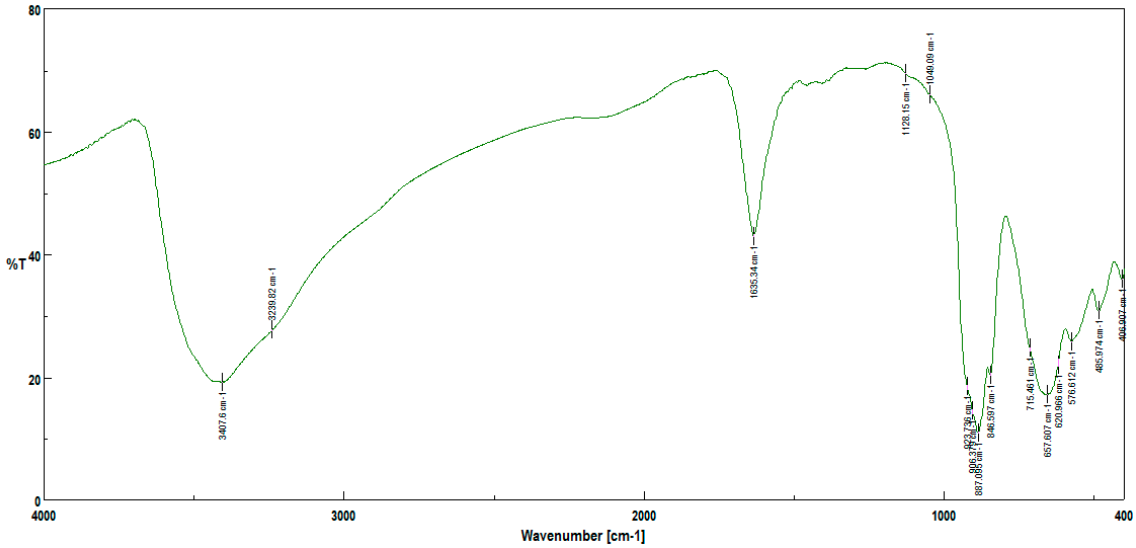

Figure S11. FTIR spectrum of POM 3, $Na_8[SiW_{11}O_{39}]\cdot 12H_2O$

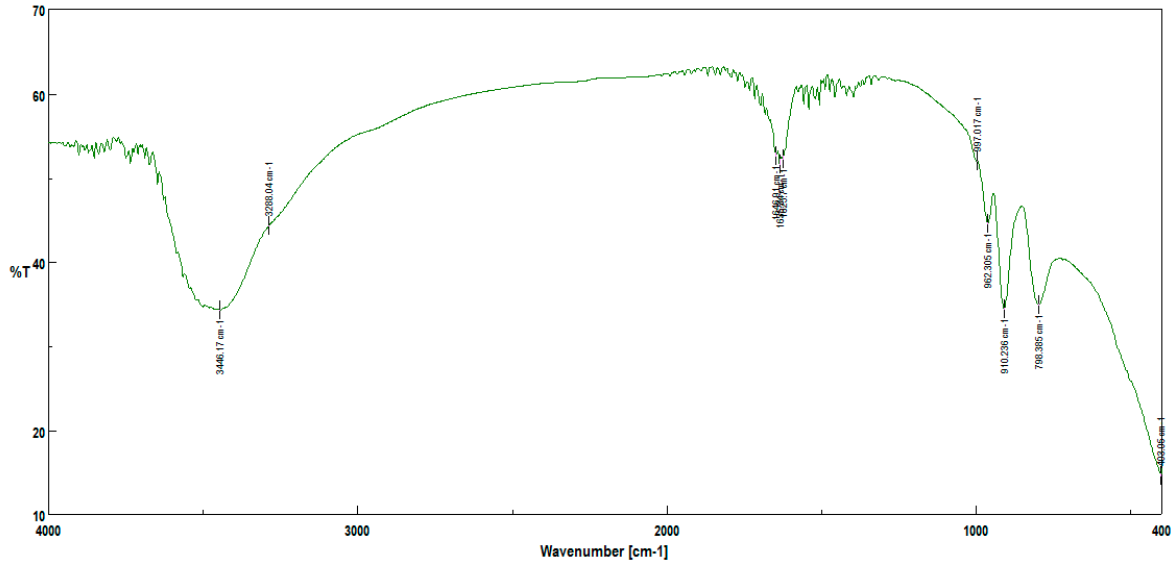

Figure S12. FTIR spectrum of POM 23a,b, $Na_5[Fe^{III}(H_2O)SiW_{11}O_{39}]\cdot 24H_2O$

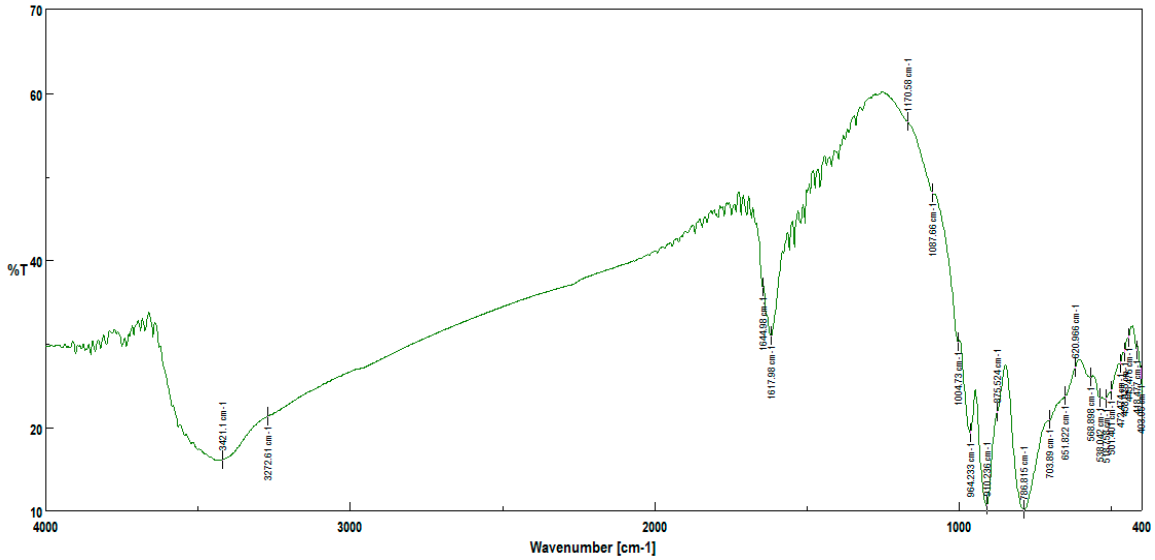

Figure S13. FTIR spectrum of POM 24a,b, $Na_5[Fe^{III}(H_2O)GeW_{11}O_{39}]\cdot 26H_2O$

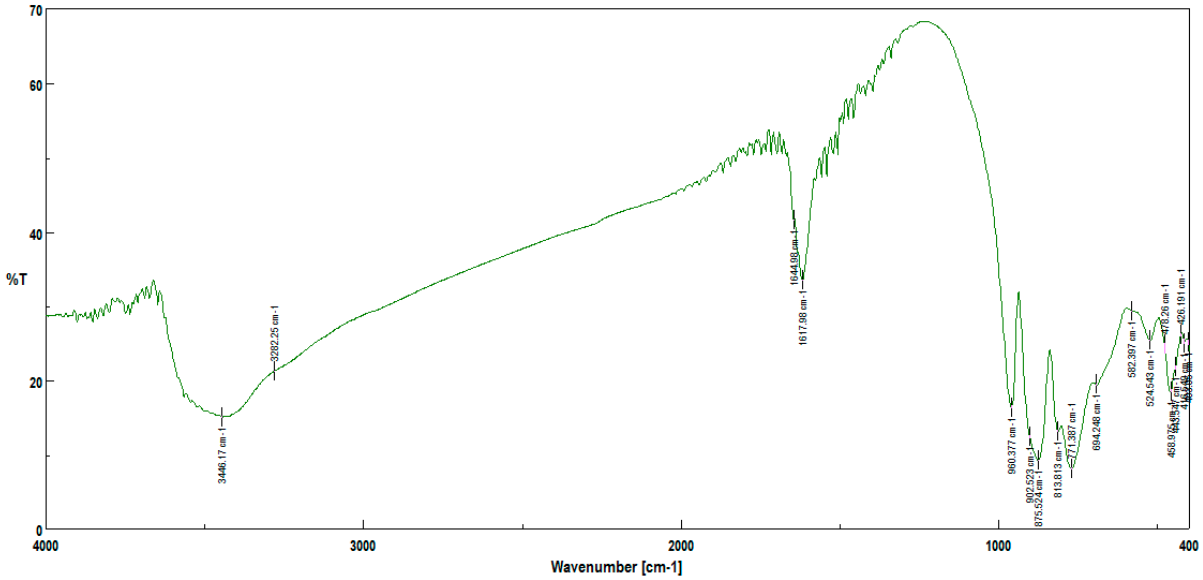

Figure S14. FTIR spectrum of POM 30, $K_6[SiV^{IV}W_{11}O_{40}]\cdot 12H_2O$

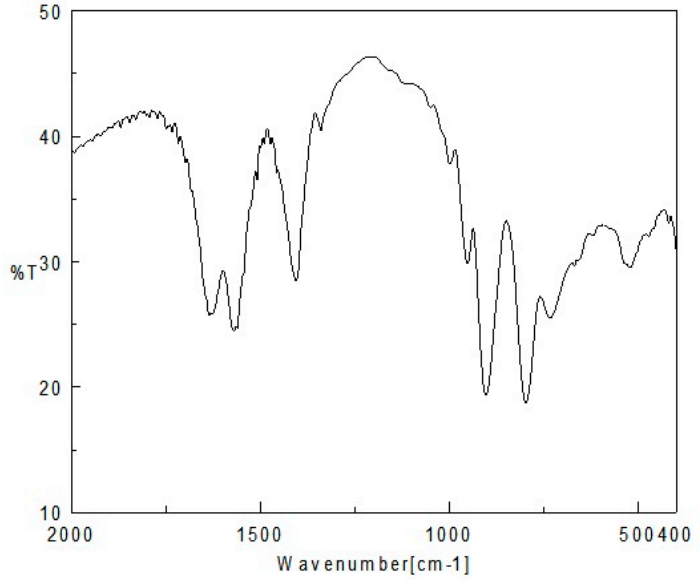

Figure S15. FTIR spectrum of POM 21, $K_6[Co(H_2O)SiMo_2W_9O_{39}]\cdot 14H_2O$, mono-lacunary Keggin with mixed addenda atoms

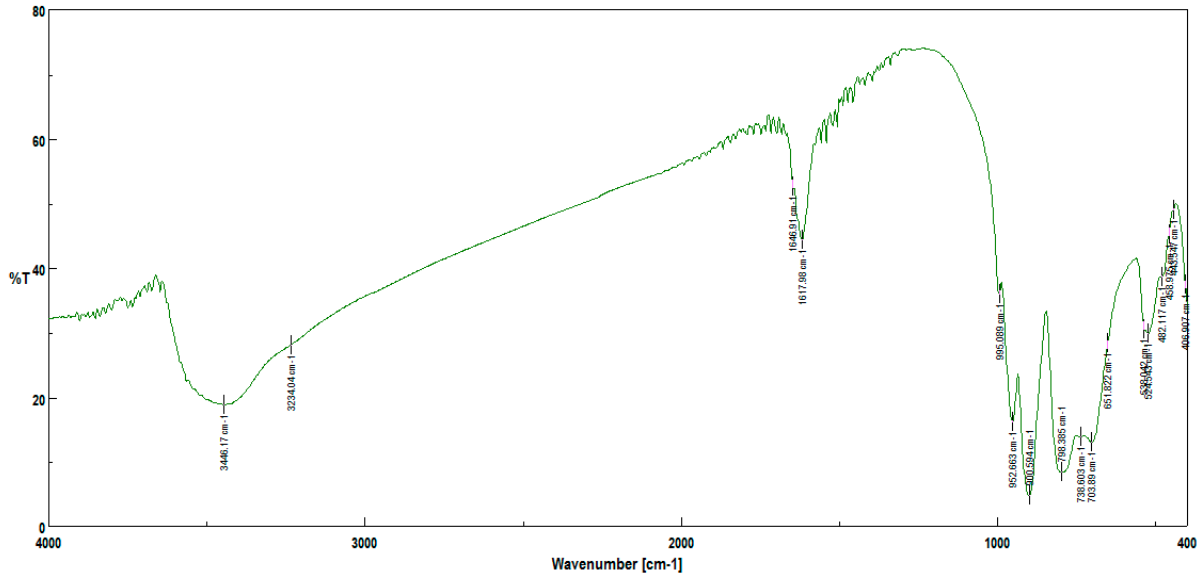

FTIR spectra of nanoPOMs with tri-lacunary Keggin structures

Figure S16. FTIR spectrum of POM 5, $K_3[(VO)_3PMo_9O_{34}]\cdot 14H_2O$

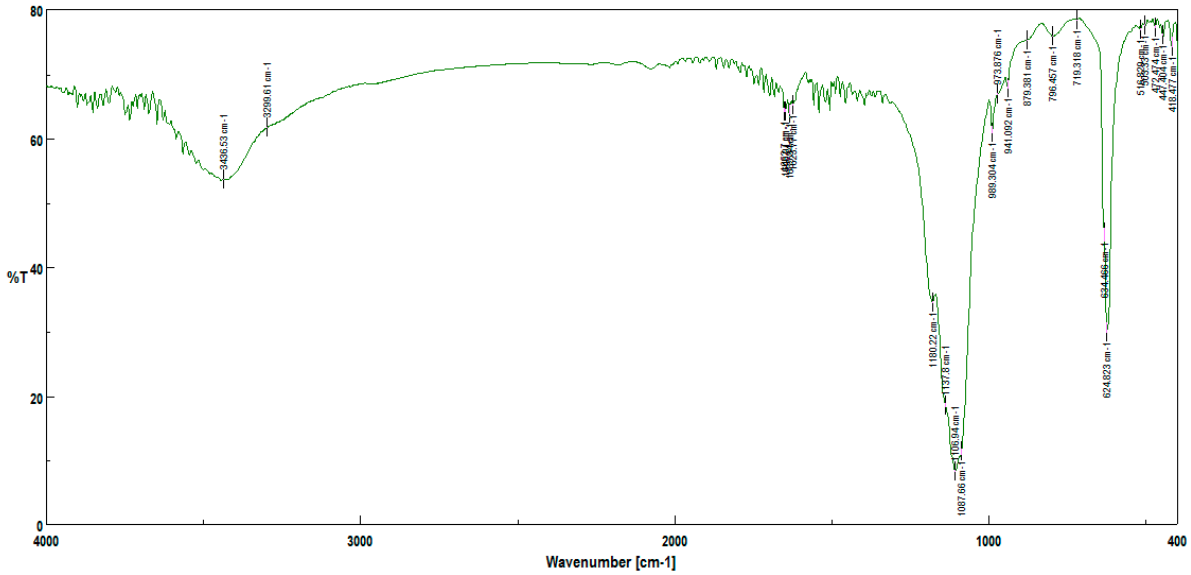

Figure S17. FTIR spectrum of POM 16a,b, $Na_{10}[SiW_9O_{34}]\cdot 24H_2O$

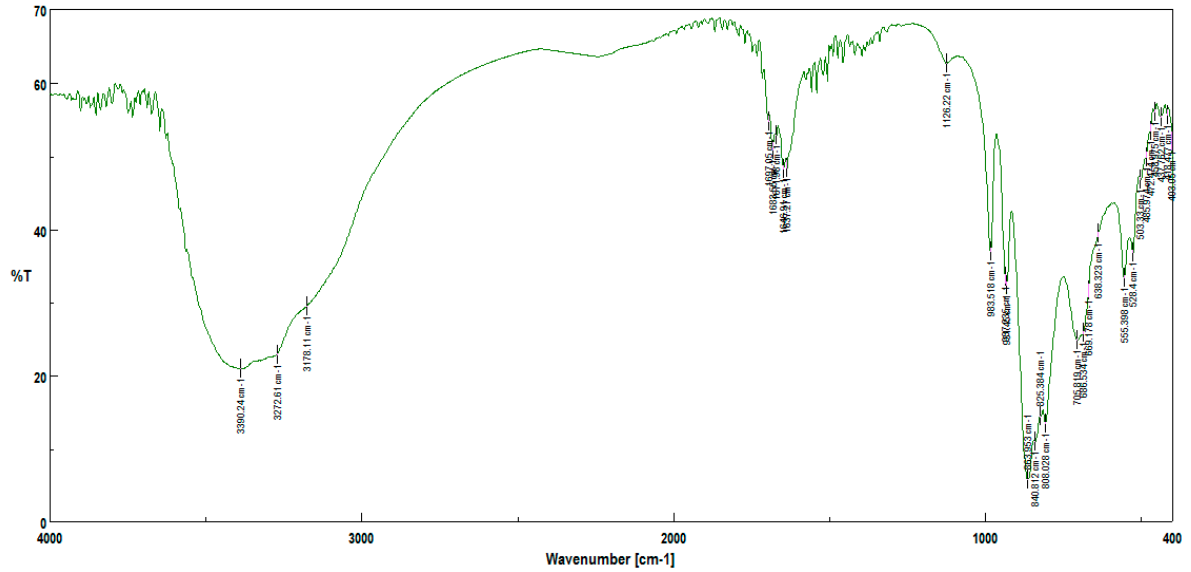

Figure S18. FTIR spectrum of POM 18, $Na_8H[PW_9O_{34}]\cdot 20H_2O$

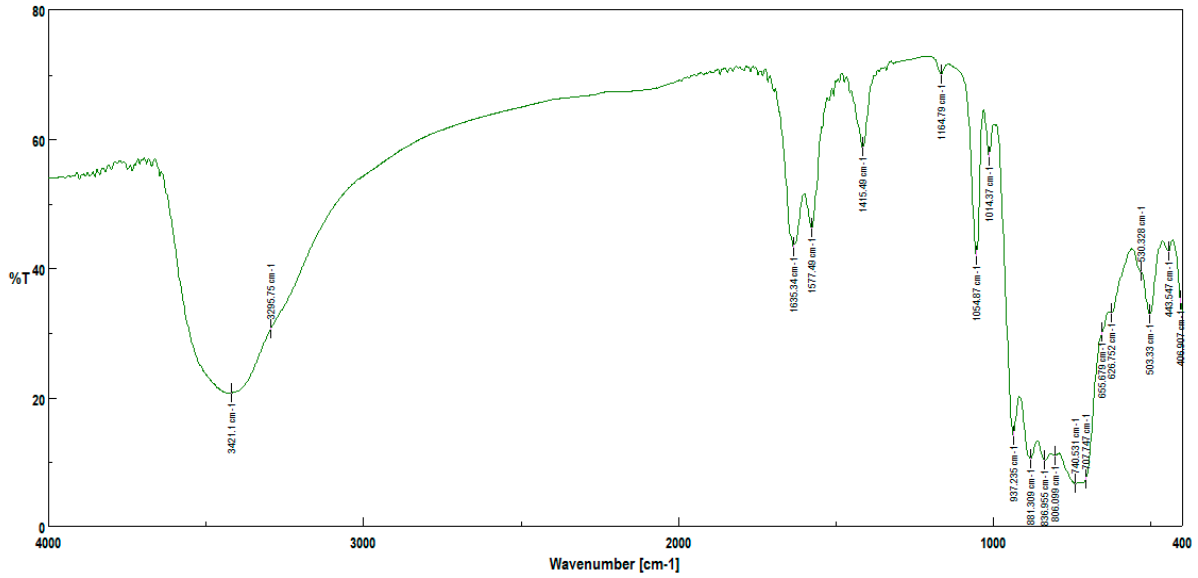

FTIR spectrum of nanoPOM with tri-lacunary *pseudo*-Keggin structures

Figure S19. FTIR spectrum of POM 15, $Na_9[SbW_9O_{33}]\cdot 19{,}5H_2O$

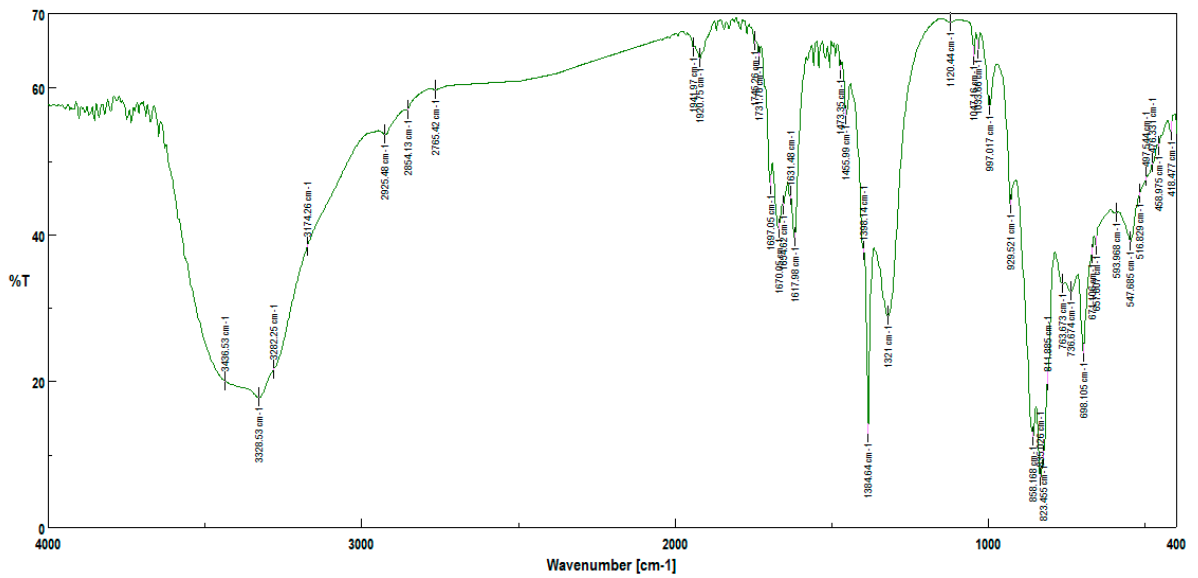

FTIR spectra of nanoPOMs with tri-lacunary Keggin/sandwich type structures

Figure S20. FTIR spectrum of POM 2, $Na_9[Fe_3(H_2O)_3(PMo_9O_{34})_2]$

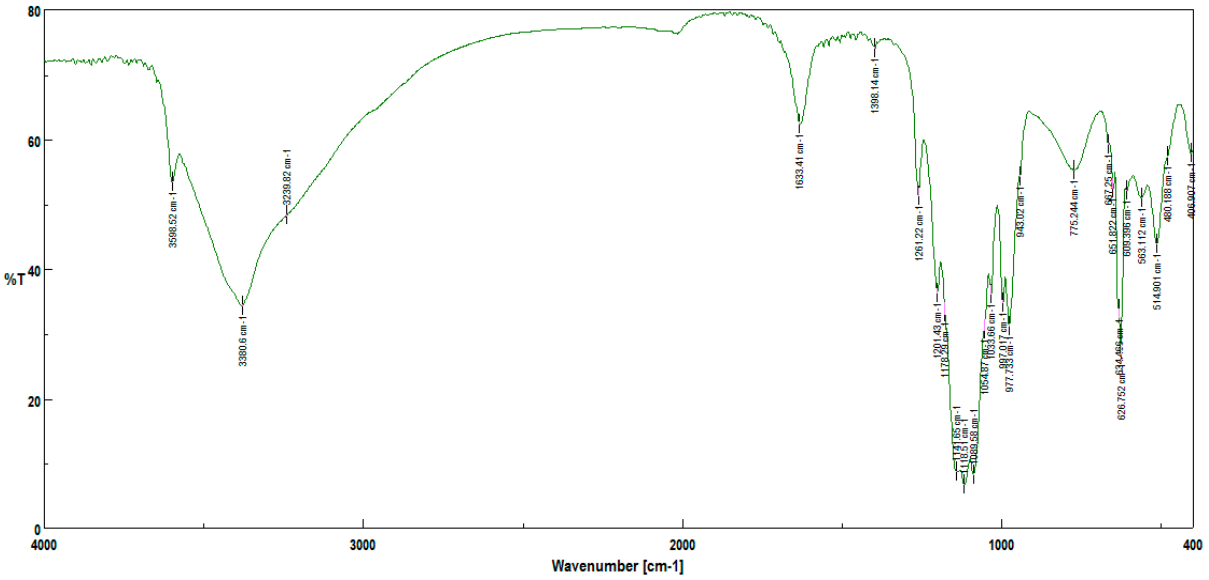

Figure S21. FTIR spectrum of POM 4, $Na_{11}[Fe_3(H_2O)_3(SiW_9O_{34})_2]\cdot 25H_2O$

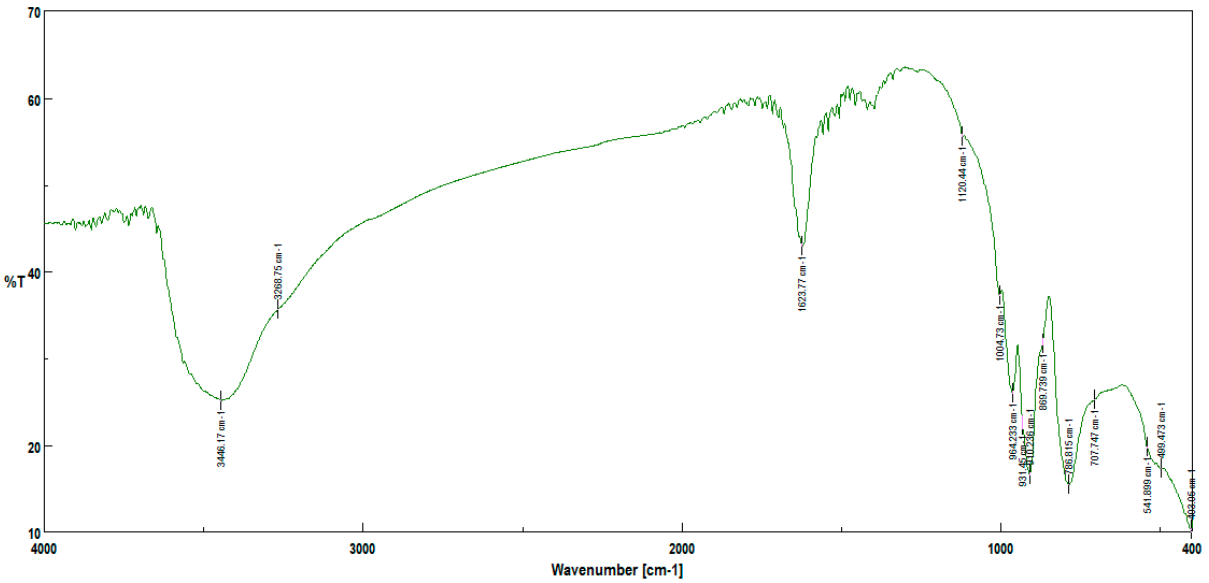

Figure S22. FTIR spectrum of POM 8, $K_{10}[(VO)_4(PW_9O_{34})_2]\cdot 26H_2O$

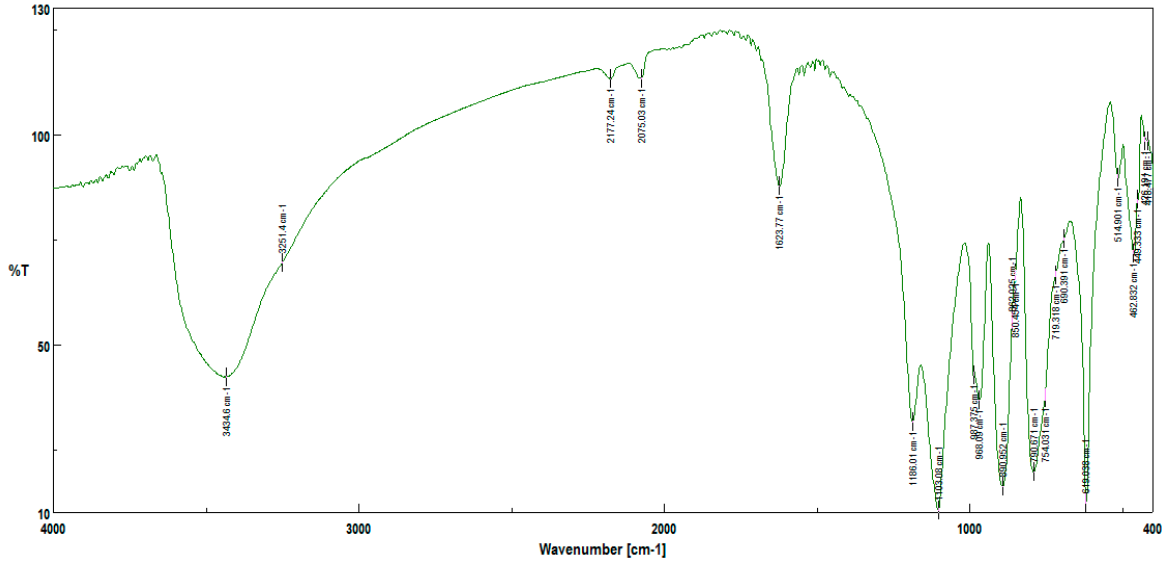

Figure S23. FTIR spectrum of POM 27, $Na_{14}[Mn_3(H_2O)_3(SiW_9O_{34})_2]\cdot 28H_2O$

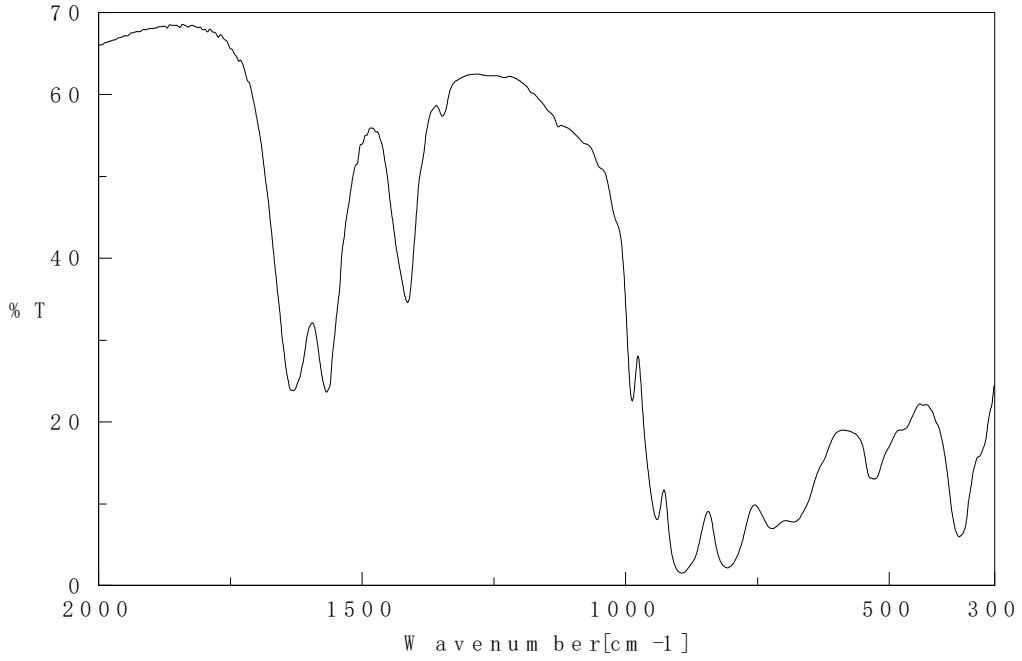

FTIR spectra of nanoPOMs with tri-lacunary *pseudo*-Keggin/sandwich type structures

FTIR spectrum of POM 10, $K_{11}H[(VO)_3(Sb^{III}W_9O_{33})_2]\cdot 27H_2O$

Published in our previous paper, cited in this paper as reference 22

Figure S24. FTIR spectrum of POM 25, $Na_{10}[Mn_4(H_2O)_2(AsW_9O_{34})_2]\cdot 27H_2O$

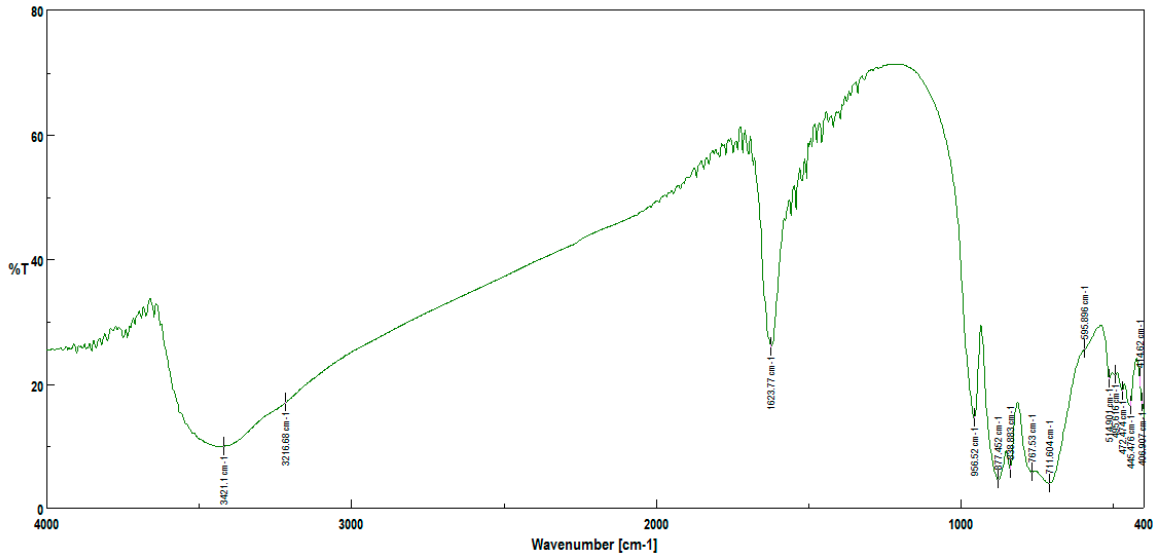

Figure S25. FTIR spectrum of POM 26, $Na_{12}[Co_3(H_2O)_3(BiW_9O_{33})_2]\cdot 37H_2O$

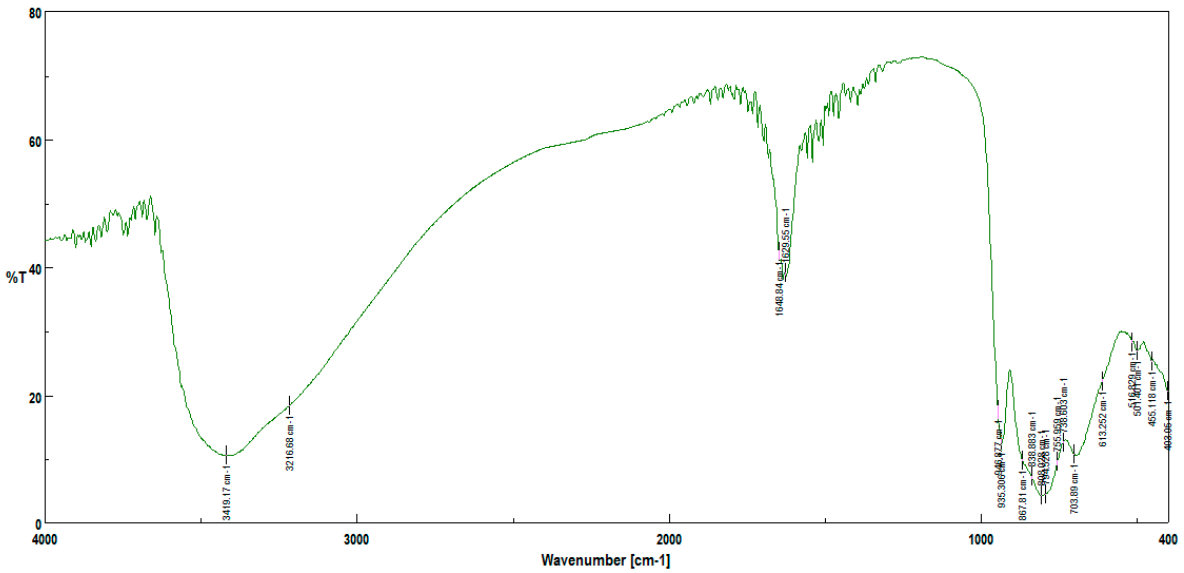

Figure S26. FTIR spectrum of POM 9, $K_{10}[(VO)_4(AsW_9O_{34})_2]\cdot 21H_2O$

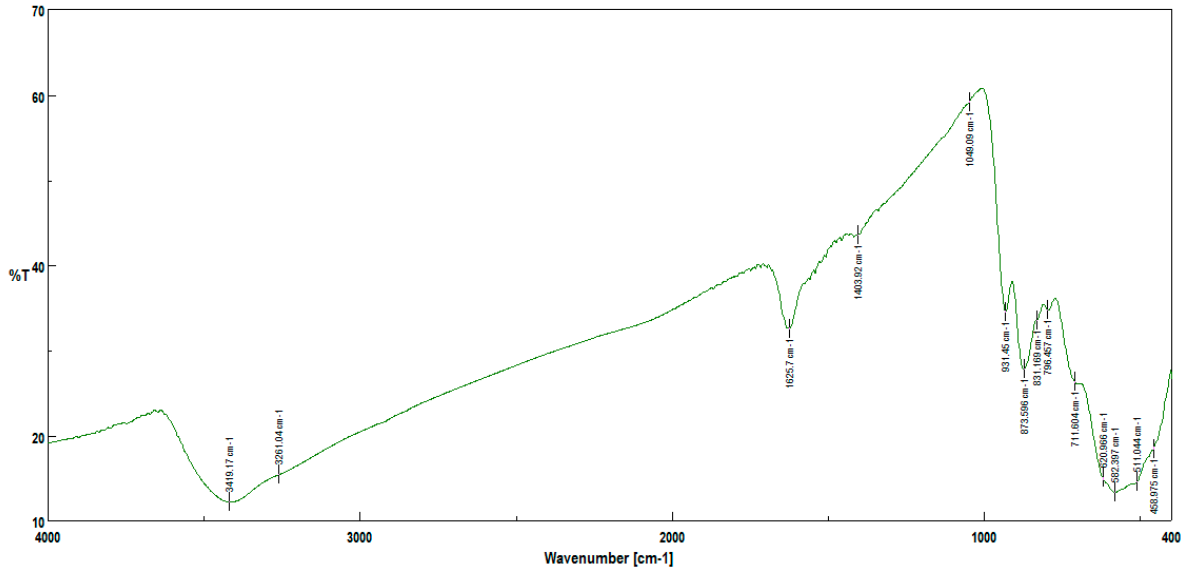

FTIR spectra of nanoPOMs with cluster structures

Figure S27. FTIR spectrum of POM 11, $Na_{12}[Sb_2W_{22}O_{74}(OH)_2]\cdot 38H_2O$

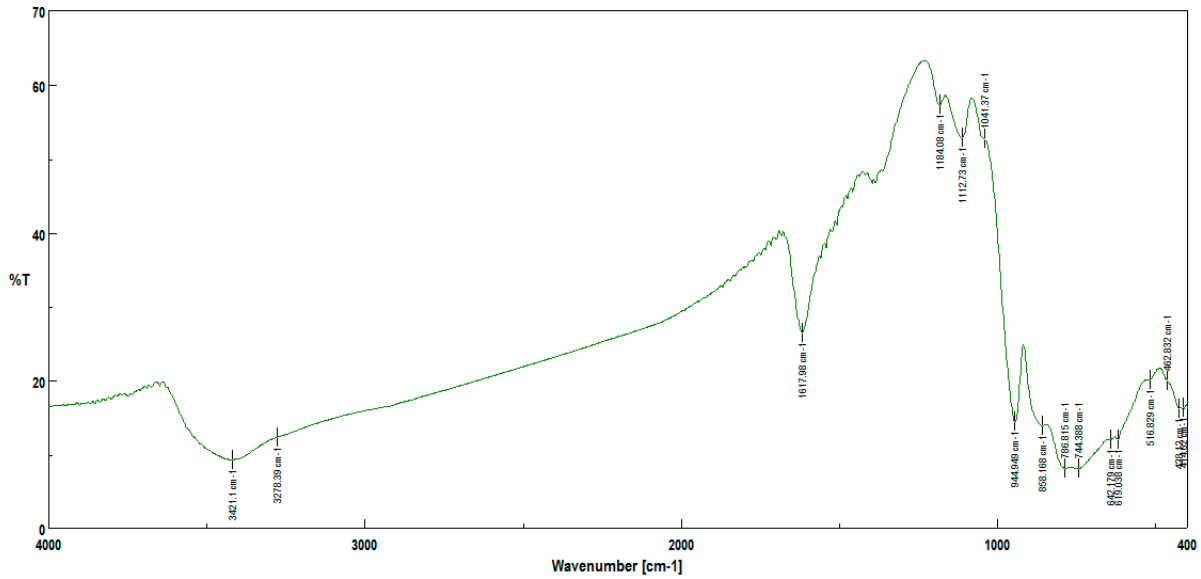

Figure S28. FTIR spectrum of POM 17, $Na_{27}[NaAs_4W_{40}O_{140}]\cdot 42H_2O$

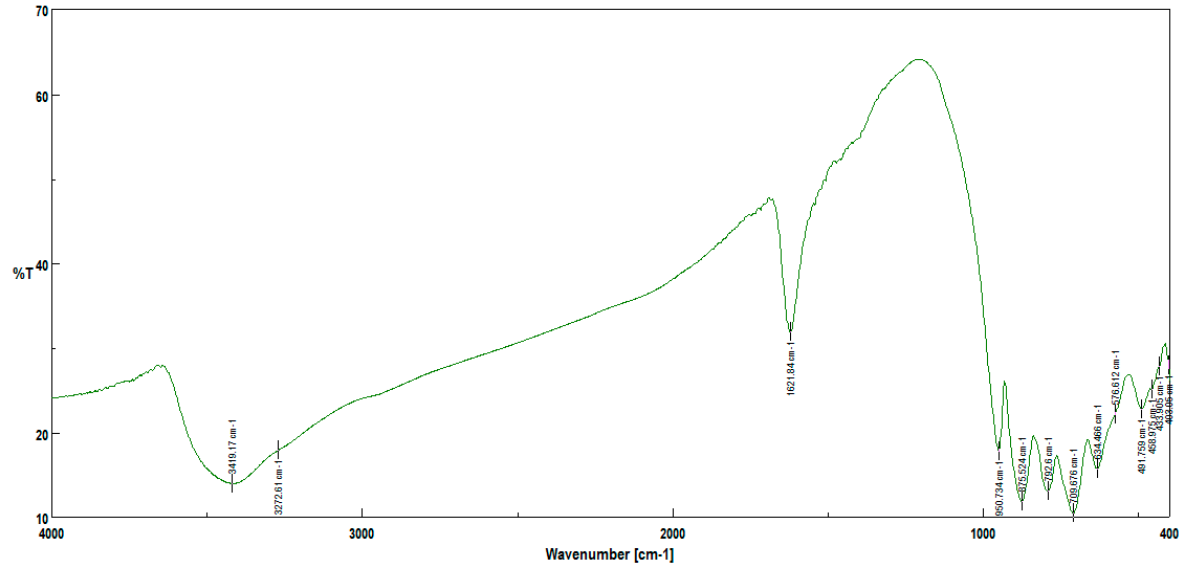

Figure S29. FTIR spectrum of POM 19, $(NBu_4)_{27}[NaAs_4Mo_{40}O_{140}]\cdot 12H_2O$

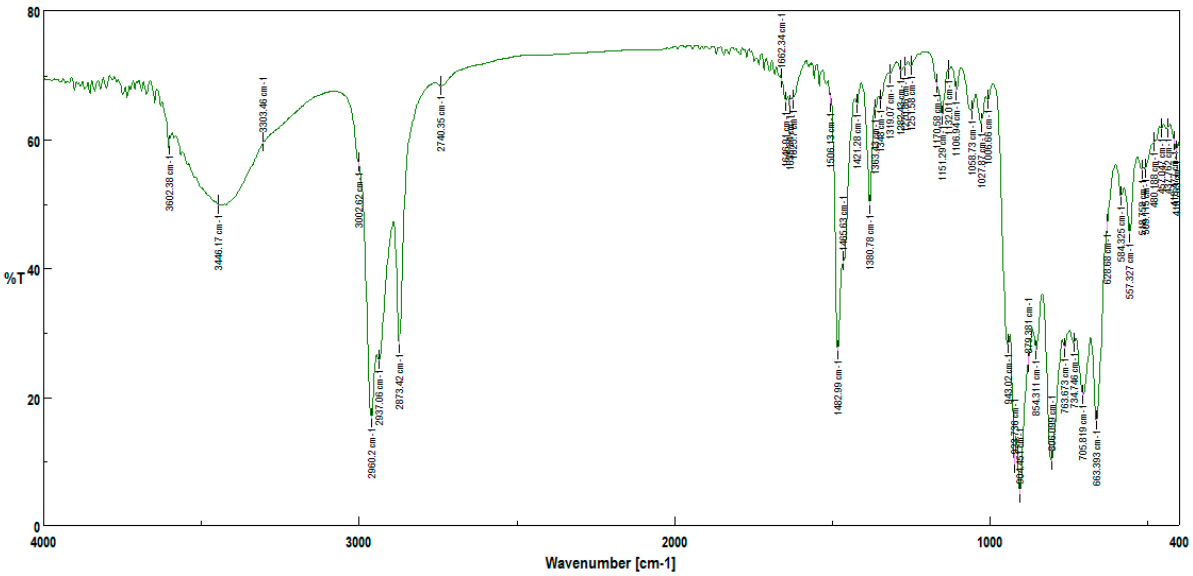

Figure S30. FTIR spectrum of POM 20, $(Bu_3Sn)_{18}[NaSb_9W_{21}O_{86}]$

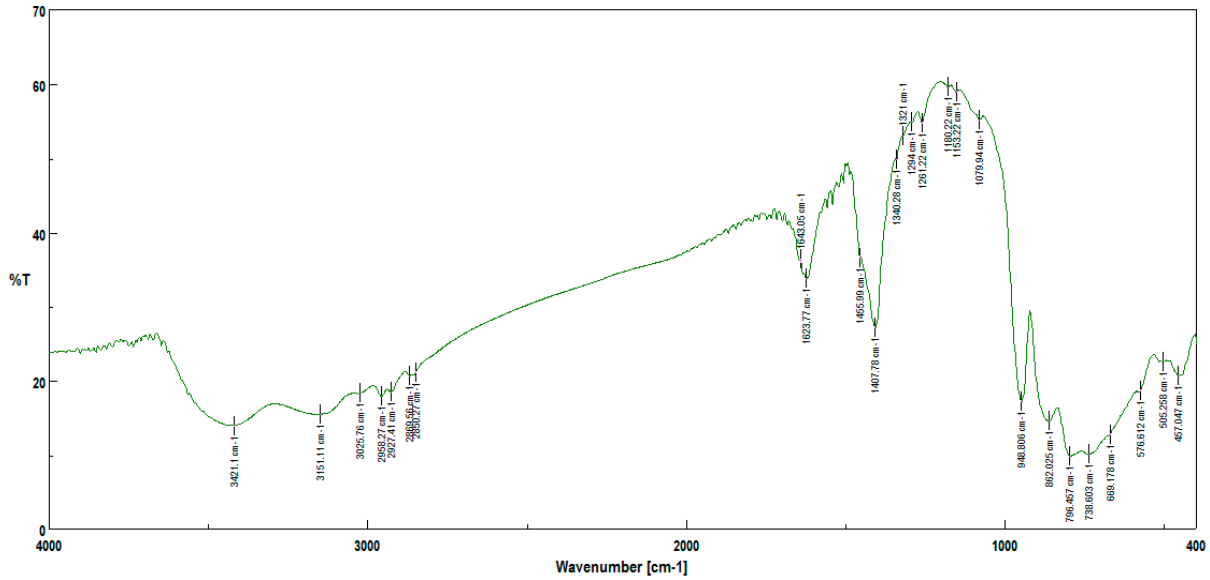

FTIR spectrum of POM 28, $(NH_4)_4(NBu_4)_5[Na(BuSn)_3Sb_9W_{21}O_{86}]\cdot 17H_2O$
Published in our previous paper, cited in this paper as reference 22

Figure S31. FTIR spectrum of POM 29, $K_{27}[NaAs_4W_{40}O_{140}]\cdot 52H_2O$

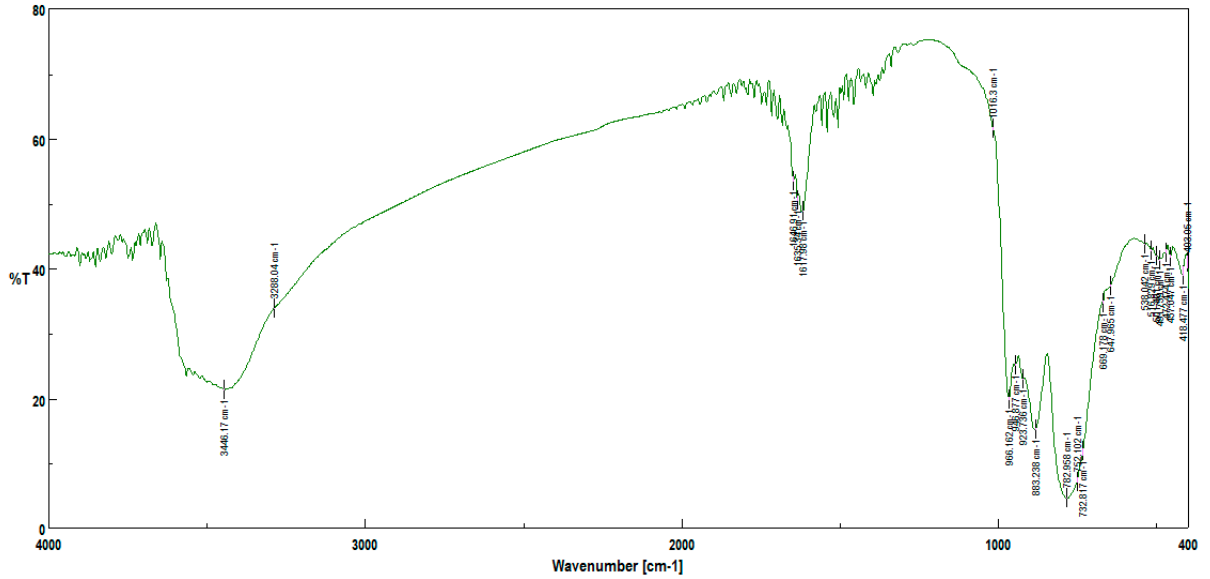

FTIR spectrum of nanoPOM, mono-lacunary Wells-Dawson with mixed addenda atoms

Figure S32. FTIR spectrum of POM 22, $K_{10}[Co(H_2O)Si_2MoW_{16}O_{61}]\cdot 18H_2O$

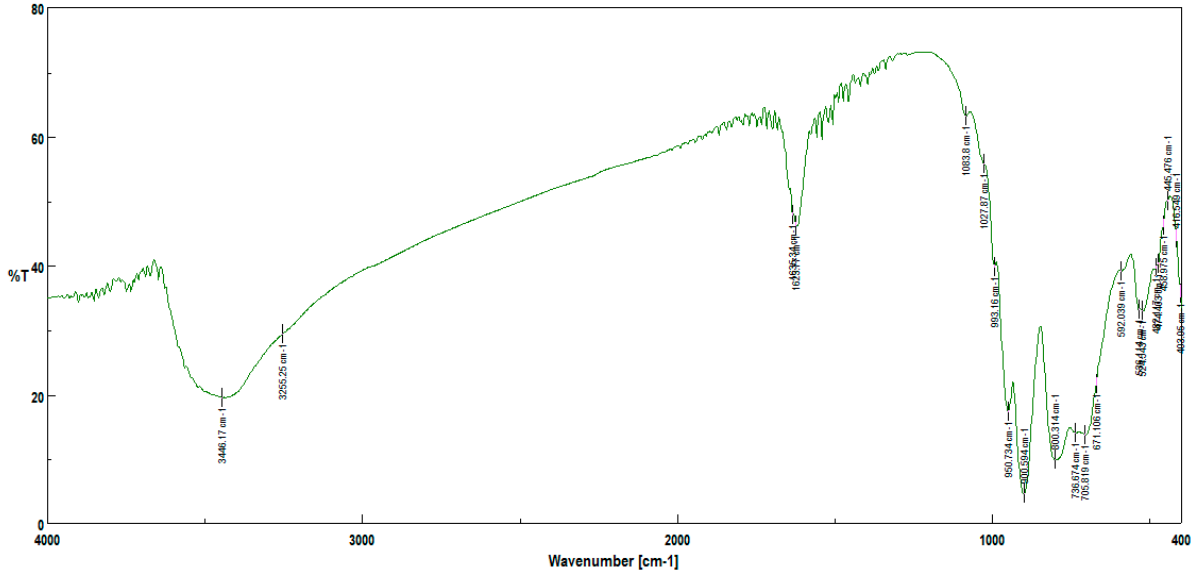

UV electronic spectra of 27 nanoPOMs

UV electronic spectra of nanoPOMs with saturated Keggin structures

Figure S33. UV electronic spectrum of POM 12, $H_4[SiW_{12}O_{40}]\cdot 14H_2O$

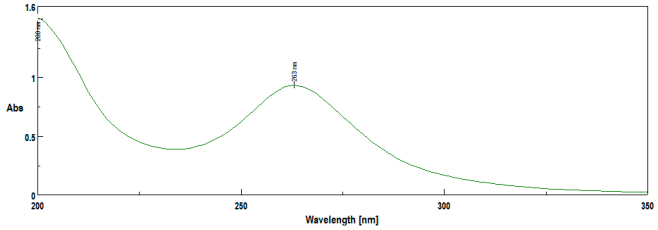

Figure S34. UV electronic spectrum of POM 13, $H_3[PW_{12}O_{40}]\cdot 12H_2O$

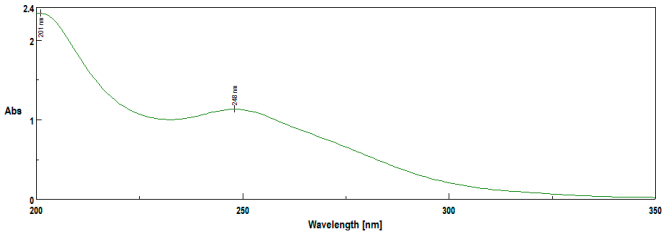

Figure S35. UV electronic spectrum of POM 14, $H_3[PMo_{12}O_{40}]\cdot 13H_2O$

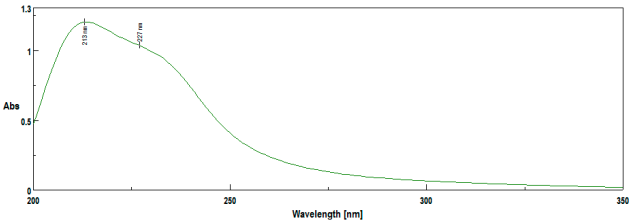

Figure S36. UV electronic spectrum of POM 6, $Na_6[PMo_9{}^{VI}V_3{}^{V}O_{40}]\cdot 16H_2O$, Keggin with mixed addenda atoms

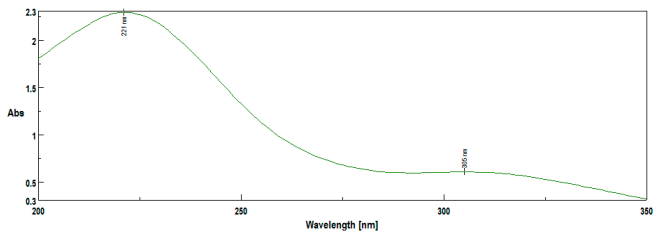

UV electronic spectra of nanoPOMs with mono-lacunary Keggin structures

Figure S37. UV electronic spectrum of POM 1, $Na_4[Fe^{III}(H_2O)PMo_{11}O_{39}]\cdot 18H_2O$

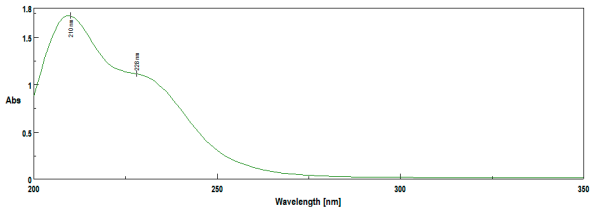

Figure S38. UV electronic spectrum of POM 3, $Na_8[SiW_{11}O_{39}]\cdot 12H_2O$

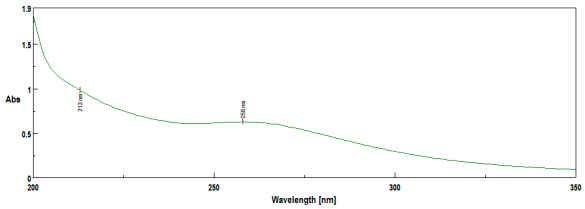

Figure S39. UV electronic spectrum of POM 23a,b, $Na_5[Fe^{III}(H_2O)SiW_{11}O_{39}]\cdot 24H_2O$

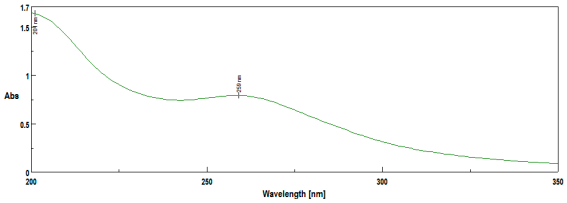

Figure S40. UV electronic spectrum of POM 24a,b, $Na_5[Fe^{III}(H_2O)GeW_{11}O_{39}]\cdot 26H_2O$

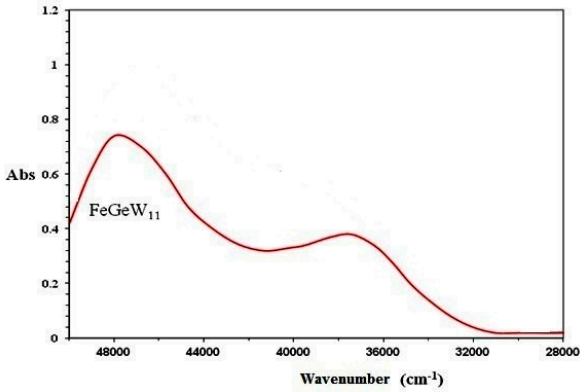

Figure S41. UV electronic spectrum of POM 30, $K_6[SiV^{IV}W_{11}O_{40}]\cdot 12H_2O$

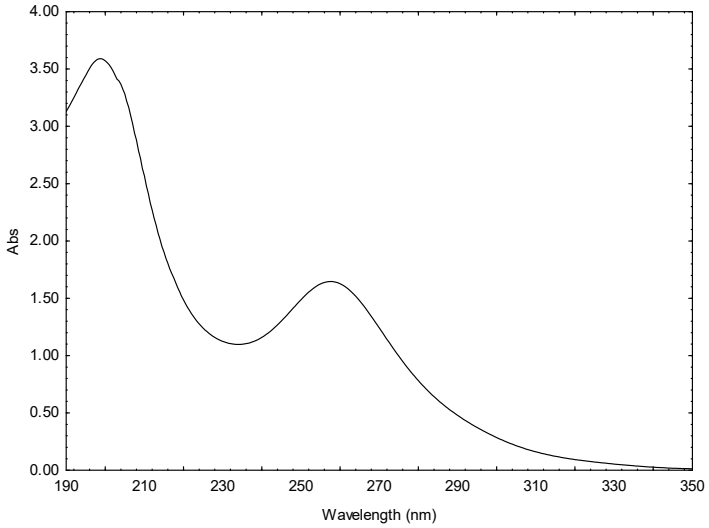

Figure S42. UV electronic spectrum of POM 21, $K_6[Co(H_2O)SiMo_2W_9O_{39}]\cdot 14H_2O$, mono-lacunary Keggin with mixed addenda atoms

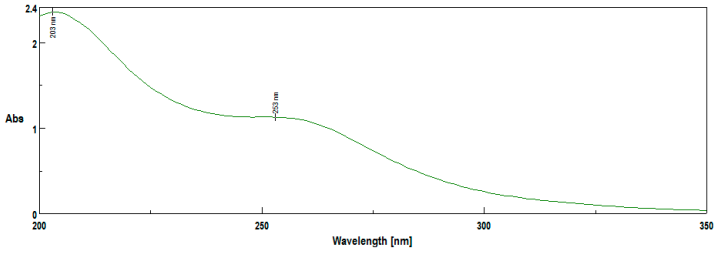

UV electronic spectra of nanoPOMs with tri-lacunary Keggin structures

Figure S43. UV electronic spectrum of POM 5, $K_3[(VO)_3PMo_9O_{34}]\cdot 14H_2O$

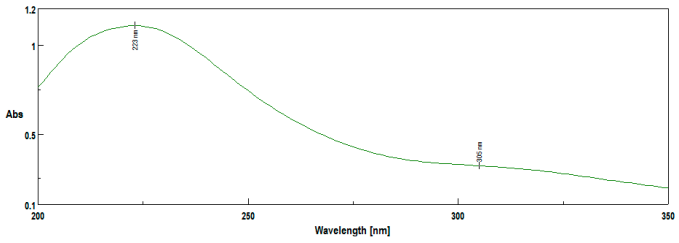

Figure S44. UV electronic spectrum of POM 16a,b, $Na_{10}[SiW_9O_{34}]\cdot 24H_2O$

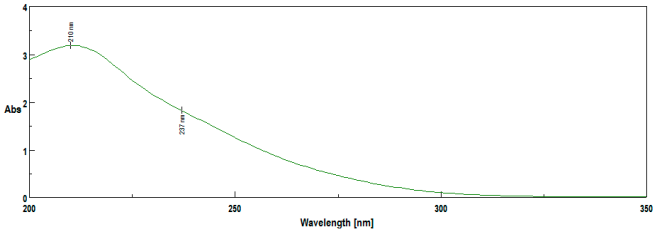

Figure S45. UV electronic spectrum of POM 18, $Na_8H[PW_9O_{34}]\cdot 20H_2O$

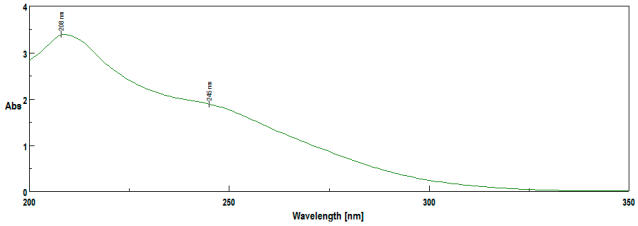

UV electronic spectrum of nanoPOM with tri-lacunary *pseudo*-Keggin structures

Figure S46. UV electronic spectrum of POM 15, $Na_9[SbW_9O_{33}]\cdot 19{,}5H_2O$

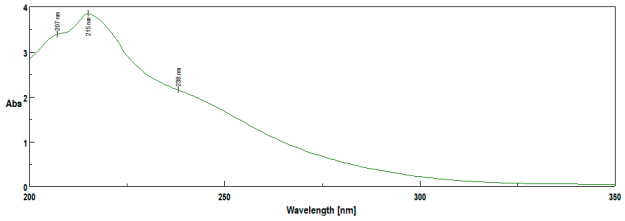

UV electronic spectra of nanoPOMs with tri-lacunary Keggin/sandwich type structures

Figure S47. UV electronic spectrum of POM 2, $Na_9[Fe_3(H_2O)_3(PMo_9O_{34})_2]$

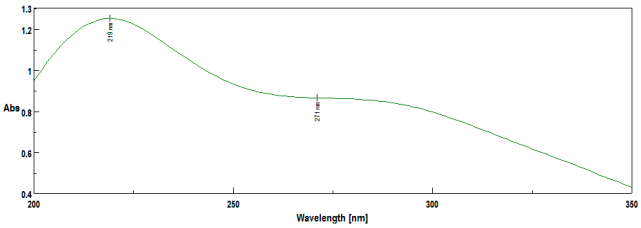

Figure S48. UV electronic spectrum of POM 4, $Na_{11}[Fe_3(H_2O)_3(SiW_9O_{34})_2]\cdot 25H_2O$

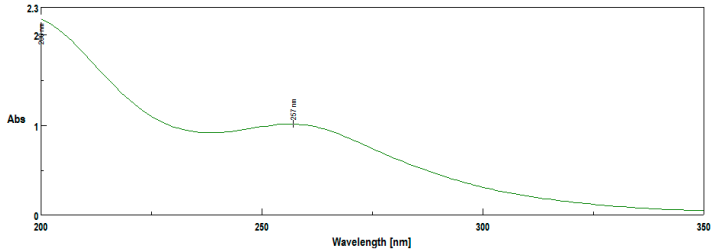

Figure S49. UV electronic spectrum of POM 8, $K_{10}[(VO)_4(PW_9O_{34})_2]\cdot 26H_2O$

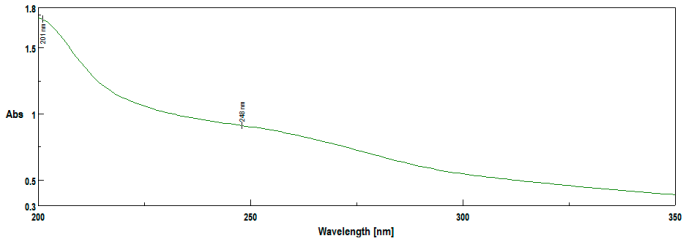

Figure S50. UV electronic spectrum of POM 27, $Na_{14}[Mn_3(H_2O)_3(SiW_9O_{34})_2]\cdot 28H_2O$

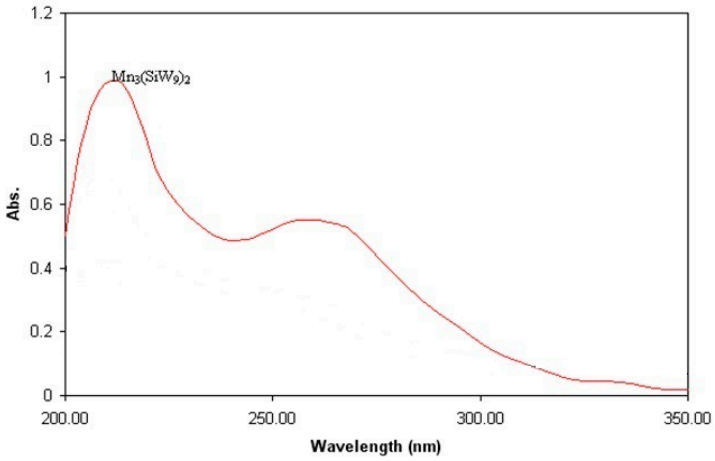

UV electronic spectra of nanoPOMs with tri-lacunary *pseudo*-Keggin/sandwich type structures

UV electronic spectrum of POM 10, $K_{11}H[(VO)_3(Sb^{III}W_9O_{33})_2]\cdot 27H_2O$

Published in our previous paper, cited in this paper as reference 22

Figure S51. UV electronic spectrum of POM 25, $Na_{10}[Mn_4(H_2O)_2(AsW_9O_{34})_2]\cdot 27H_2O$

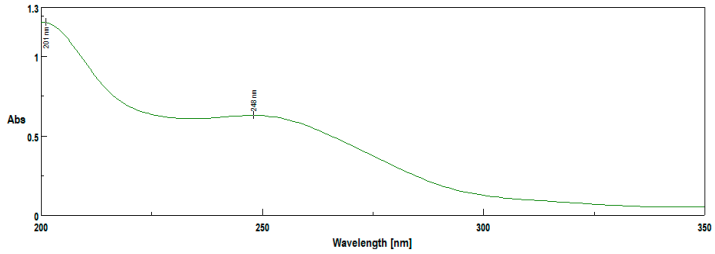

Figure S52. UV electronic spectrum of POM 26, $Na_{12}[Co_3(H_2O)_3(BiW_9O_{33})_2]\cdot 37H_2O$

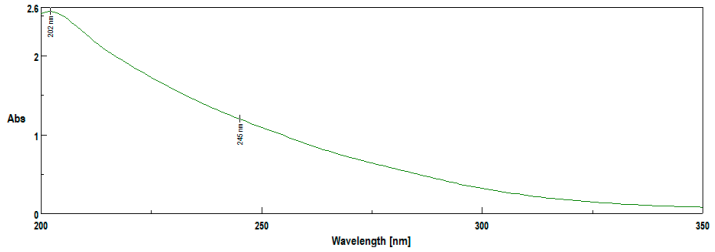

Figure S53. UV electronic spectrum of POM 9, $K_{10}[(VO)_4(AsW_9O_{34})_2]\cdot 21H_2O$

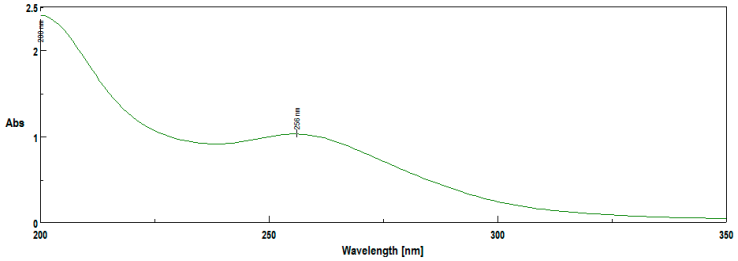

UV electronic spectra of nanoPOMs with cluster structures

Figure S54. UV electronic spectrum of POM 11, $Na_{12}[Sb_2W_{22}O_{74}(OH)_2]\cdot 38H_2O$

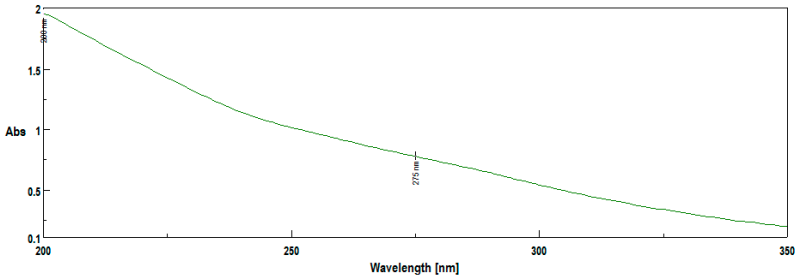

Figure S55. UV electronic spectrum of POM 17, $Na_{27}[NaAs_4W_{40}O_{140}]\cdot 42H_2O$

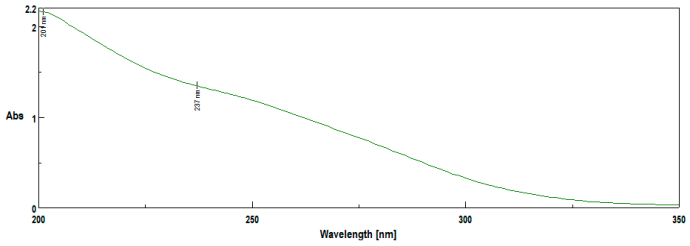

Figure S56. UV electronic spectrum of POM 19, $(NBu_4)_{27}[NaAs_4Mo_{40}O_{140}]\cdot 12H_2O$

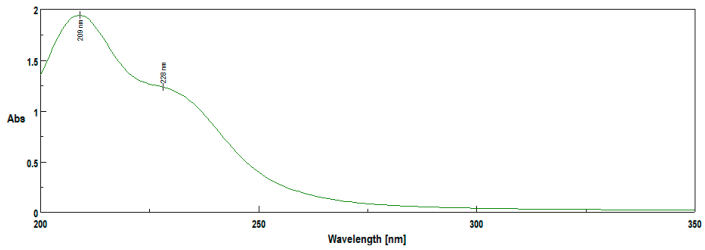

Figure S57. UV electronic spectrum of POM 20, $(Bu_3Sn)_{18}[NaSb_9W_{21}O_{86}]$

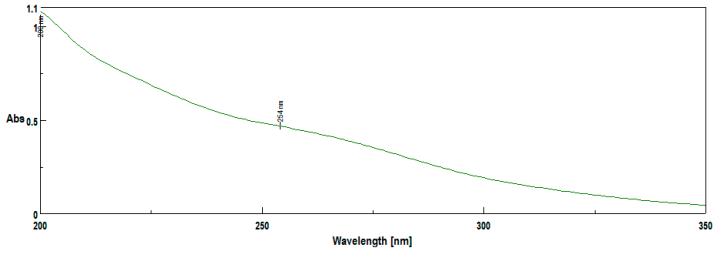

UV electronic spectrum of POM 28, $(NH_4)_4(NBu_4)_5[Na(BuSn)_3Sb_9W_{21}O_{86}]\cdot 17H_2O$
Published in our previous paper, cited in this paper as reference 22

Figure S58. UV electronic spectrum of POM 29, $K_{27}[NaAs_4W_{40}O_{140}]\cdot 52H_2O$

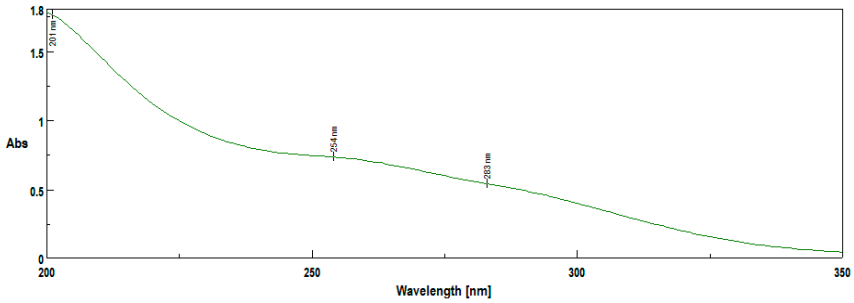

<u>UV electronic spectrum of nanoPOM mono-lacunary Wells-Dawson with mixed addenda atoms</u>

Figure S59. UV electronic spectrum of POM 22, $K_{10}[Co(H_2O)Si_2MoW_{16}O_{61}]\cdot 18H_2O$

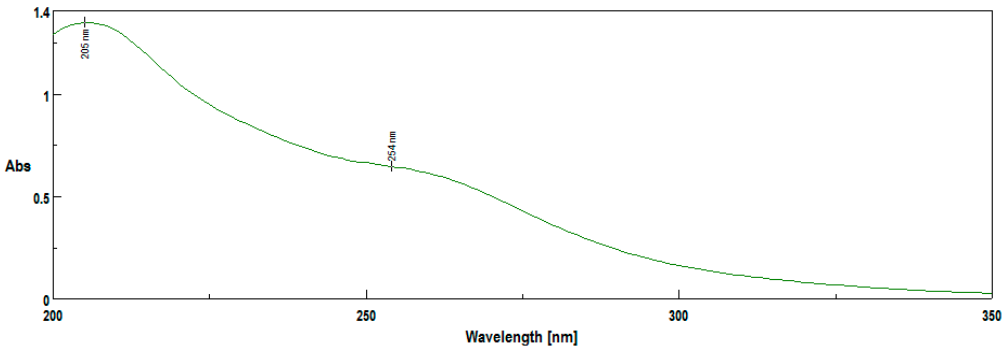

Bacterial inoculi microplates prepared from various reference strains inhibited by the 21 analyzed nanoPOMs

Figure S60. Inhibition aspects for the 21 nanoPOMs analyzed (in microplates of bacterial inoculum prepared from reference strain ATCC 6538P – *Staphylococcus aureus*):
A-C. Active nanoPOMs, D. Control samples.

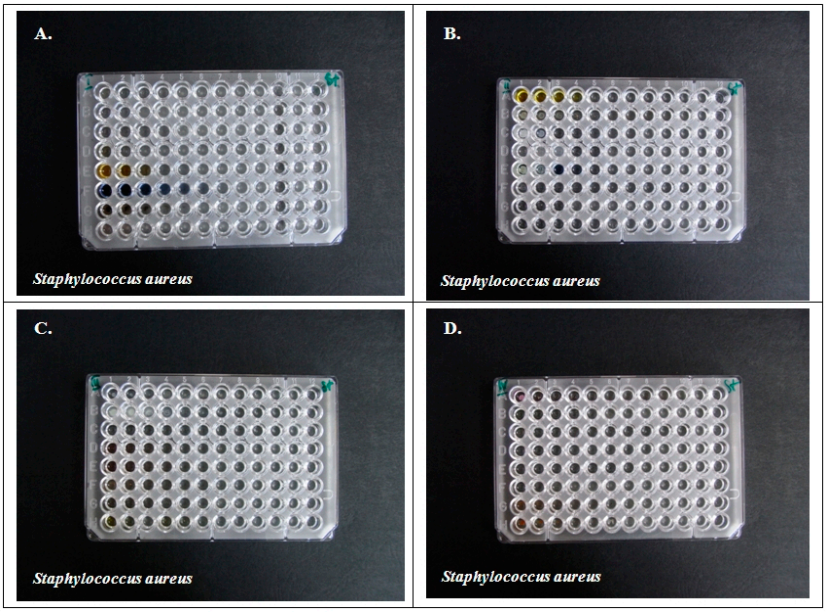

Figure S61. Inhibition aspects for the 21 nanoPOMs analyzed (in microplates of bacterial inoculum prepared from reference strain ATCC 14579 – *Bacillus cereus*):
A-C. Active nanoPOMs, D. Control samples.

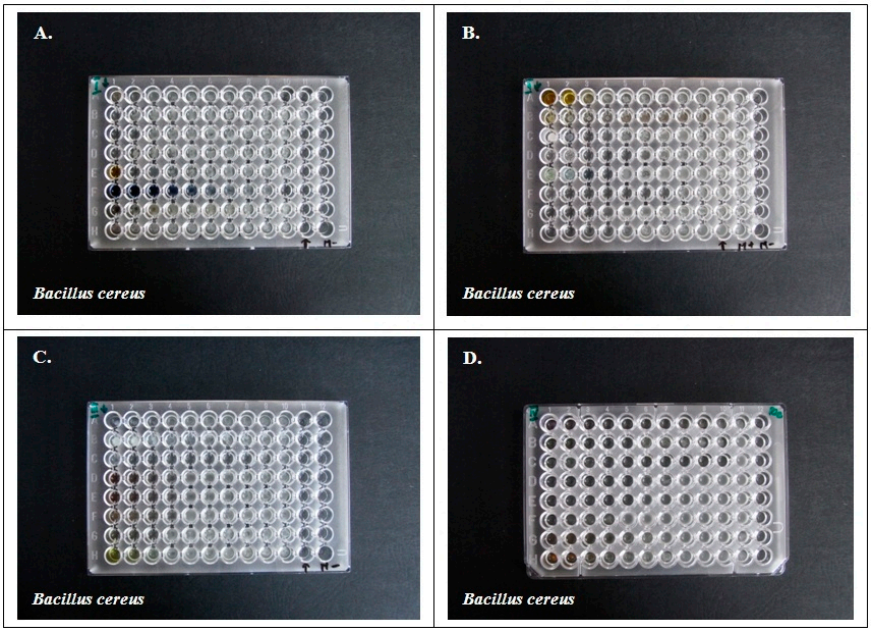

Figure S62. Inhibition aspects for the 21 nanoPOMs analyzed (in microplates of bacterial inoculum prepared from reference strain ATCC 13076 – *Salmonella enteritidis*):
A-C. Active nanoPOMs, D. Control samples.

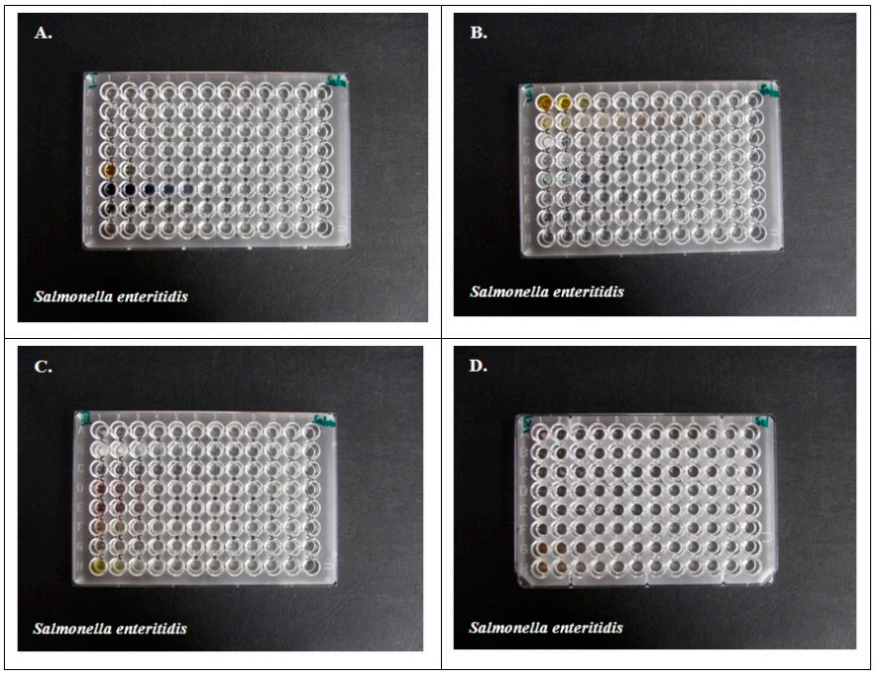

Figure S63. Inhibition aspects for the 21 nanoPOMs analyzed (in microplates of bacterial inoculum prepared from reference strain ATCC 10536 – *Escherichia coli*):
A-C. Active nanoPOMs, D. Control samples.

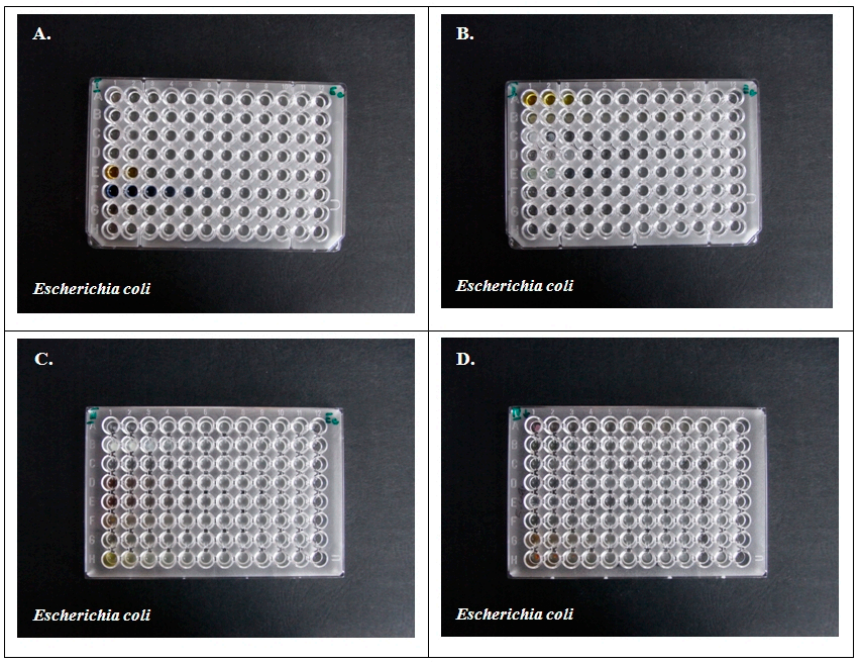

Figure S64. Inhibition aspects for the 21 nanoPOMs analyzed (in microplates of bacterial inoculum prepared from reference strain ATCC 27853 – *Pseudomonas aeruginosa*): A-C. Active nanoPOMs, D. Control samples.